VOLUME 32 NUMBER 2 April 2026
pISSN 2287-2728
eISSN 2387-285X

CLINICAL and MOLECULAR HEPATOLOGY

The forum for latest knowledge of hepatobiliary diseases

CV outcomes of oral antidiabetics in MASLD

Network meta-analysis of liver transplant criteria
ERBB3 blockade sensitizes HCC to regorafenib
ACSS2 as a metabolic target in HBV-related HCC

KASL

pISSN 2287-2728
eISSN 2287-285X

Clinical & Molecular Hepatology

https://doi.org/10.3350/cmh.2025.1370
Clinical and Molecular Hepatology 2026;32:808-828

Original Article

FOXM1 influences DNA methylation to augment *TACC3* alternative splicing directed by KAT2A in hepatocellular carcinoma

Li Na Zhao and Jesper B. Andersen

Department of Health and Medical Sciences, Biotech Research and Innovation Centre (BRIC), University of Copenhagen, Copenhagen, Denmark

Graphical Abstract

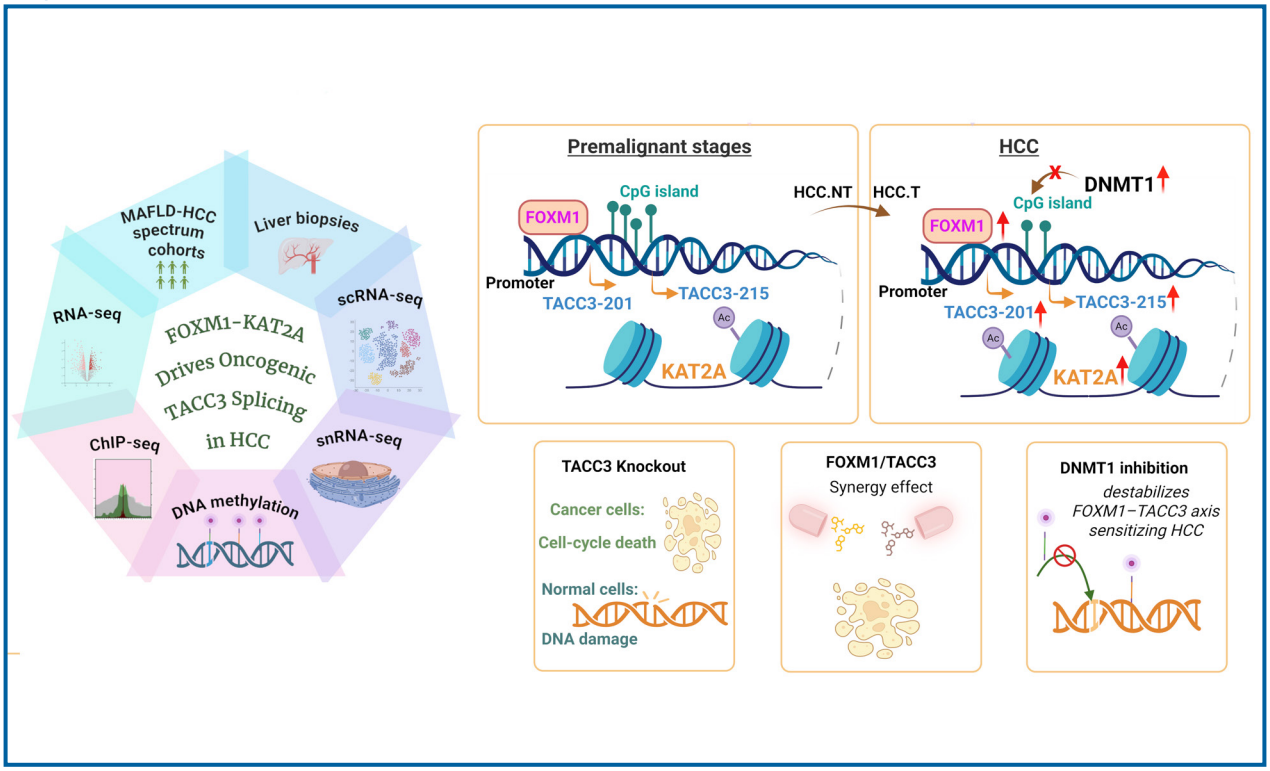

Study Highlights

- *FOXM1* overrides *DNMT1* to activate *TACC3* via KAT2A-CpG-defined chromatin remodeling.
- TACC3-KAT2A interaction with alternative splicing (AS) switches from NOTCH4 regulation (non-cancerous tissue) to cell-cycle promotion (tumor).
- *TACC3* knockdown selectively targets cancer cells (p53-PUMA-mediated apoptosis) over normal tissue (DNA repair only).

Background/Aims: Hepatocellular carcinoma (HCC) is characterized by profound transcriptomic dysregulation, yet the mechanism(s) by which DNA methylation is coordinated with chromatin modifications to regulate alternative splicing during tumorigenesis remains poorly understood.

Methods: Using prospectively paired multi-omics data obtained from metabolic dysfunction-associated steatotic liver disease (MASLD)-HCC patients and coupled with a premalignant MASLD cohort, we have uncovered a previously unrecognized gene-regulatory axis centered on TACC3 isoform-switching.

Results: In the non-tumoral context, the TACC3-201 isoform directly engages the histone acetyltransferase *KAT2A* to coordinate the regulation of NOTCH4 signaling. In HCC, this regulatory axis is disrupted whereby *FOXM1* overrides DNMT1-mediated methylation, upregulating *TACC3*, and decoupling *TACC3* from the KAT2A-associated NOTCH4 co-expression module. This rewiring is licensing tumor-specific cell-cycle progression and epigenetic plasticity. Thus, *FOXM1* reshapes the TACC3-KAT2A interaction, while DNMT1 drives context-dependent DNA methylation, activating the CDK1-inhibitory kinase PKMYT1.

Conclusions: We uncovered TACC3-KAT2A as an emerging regulatory axis caused by alternative splicing in HCC and propose FOXM1-driven TACC3 inhibition to synergistically disrupt mitotic fidelity and transcriptional regulation, potentially offering new therapeutic avenues for HCC with reduced toxicity to the normal liver. **(Clin Mol Hepatol 2026;32:808-828)**

Keywords: Hepatocellular carcinoma; Alternative splicing; *TACC3*; *KAT2A*; *FOXM1*

INTRODUCTION

Hepatocellular carcinoma (HCC) develops via cumulative genetic and epigenetic disruptions, with recent transcriptome-wide studies implicating alternative splicing (AS) in over 30% of tumors.[1-3] However, the mechanisms linking chromatin state, DNA methylation, and isoform-switching remain poorly understood. Specifically, it remains unclear how the histone 3 lysine 9 acetylation (H3K9ac) state, regulated by lysine acetyltransferase 2A (*KAT2A*) and DNA methyltransferase 1 (DNMT1), are rewired to influence alternative promoter usage and exon inclusion in HCC.[4] Moreover, the extent to which transcription factors, such as *FOXM1*, reprogram the interplay of AS-epigenetic networks to drive isoform-specific expression and the downstream consequences of isoform-switching on immune evasion remain elusive, limiting our understanding of how AS shapes tumor progression.

Recent evidence suggests that isoform diversity, driven by AS, contributes functionally to HCC progression.[5,6] Notably, transforming acidic coiled-coil containing protein 3 (*TACC3*), a key player in mitotic progression and centrosome stability, exhibits complex splicing patterns in cancer.[7] Although TACC3 is a known regulator in tumorigenesis in many cancers,[7-9] its isoform-specific functionality and epigenetic regulation remain poorly understood.

Corresponding author : **Jesper B. Andersen**
Department of Health and Medical Sciences, Biotech Research and Innovation Centre (BRIC), University of Copenhagen, Ole Maaløes Vej 5, Copenhagen N, DK-2200 Denmark
Tel: +45 35325834, E-mail: jesper.andersen@bric.ku.dk
https://orcid.org/0000-0003-1760-5244

Editor: Murim Choi, Department of Biomedical Sciences, Seoul National University College of Medicine, Korea **Received :** Dec. 10, 2025 / **Revised :** Jan. 6, 2026 / **Accepted :** Jan. 23, 2026

Abbreviations:

AS, alternative splicing; ATSS, alternative transcription start site; ATTS, alternative transcription termination site; DNMT1, DNA methyltransferase 1; FOXM1, Forkhead box protein M1; HCC, hepatocellular carcinoma; hdWGCNA, high-dimensional WGCNA; H3K9ac, histone 3 lysine 9 acetylation; KAT2A, lysine acetyltransferase 2A; NMD, nonmediated decay; PLS, partial least squares; snRNA-seq, single nucleus RNA sequencing; TACC3, transforming acidic coiled-coil containing protein 3; TR, transcription regulator; WGCNA, weighted gene co-expression network analysis

DNMT1 is the principal maintenance DNA methyltransferase that propagates DNA methylation during cell division to preserve transcriptional silencing.[10] Despite being consistently overexpressed in HCC and other malignancies, DNMT1 inhibitors induce significant hepatotoxicity and have shown limited therapeutic efficacy in solid tumors, which likely is due to context-specific resistance and compensatory epigenetic mechanisms.[11,12] Importantly, DNMT1 does not act in isolation; rather, it operates within chromatin contexts shaped by histone modifications, DNA accessibility, and interactions with regulatory cofactors.[13,14] These dynamics are critical for understanding why some oncogenic targets, such as *TACC3*, can escape DNMT1-mediated repression, despite the involvement of DNMT1 in their epigenetic control.[15]

Moreover, Forkhead box protein M1 (*FOXM1*), a master transcriptional regulator involved in cell proliferation and genome instability in cancer,[16] has been implicated in controlling AS by recruiting cofactors and influencing the chromatin state.[17] Recently, it was shown in liver cancer stem cells that aberrant DNMT1 activation leads to miR-34a promoter methylation and silencing, resulting in *FOXM1* upregulation and increased cell stemness.[18] Intriguingly, *FOXM1* and *DNMT1* are both upregulated in HCC, yet their interrelated regulatory influence on transcript isoform-selection or -silencing is gene- and context-specific.[19,20]

Given this unresolved complexity, we hypothesized that *TACC3* isoforms act as molecular scaffolds, rewiring oncogenic signaling in HCC. We demonstrate a previously unrecognized AS-directed mechanism by which TACC3-201 coordinates *KAT2A* to regulate NOTCH4 signaling in non-malignant stages. In contrast, *FOXM1* disrupts this complex in HCC, overriding *DNMT1*-mediated methylation, elevating *TACC3*, and licensing cell-cycle progression.

MATERIALS AND METHODS

Patient cohorts

Prospective patient samples are obtained in two cohorts. Metabolic dysfunction-associated steatotic liver disease (MASLD) cohort (42 healthy controls, 66 individuals with MASLD, and 11 with metabolic dysfunction-associated steatohepatitis [MASH])[21] and a MASLD-HCC cohort,[22] including 47 patients with paired tumor and adjacent non-tumor tissue samples. The study was performed following individual patient consent, and local institutional review board approvals (IORG0003254; IRB00003888), and assessed by the Committee on Health and Research Ethics for the Capital Region of Denmark for use of archival material (no. H-4-2016-FSP, 17029679). All patient datasets were anonymized.

In vivo and in vitro functional validation and external datasets

Multiple publicly available datasets were used for discovery, validation, and mechanistic analysis. The discovery cohort included scRNA-seq data from paired tumor and adjacent non-tumor liver tissues of HCC patients (GSE149614).[23] Validation datasets included GSE189903[24] with tumor core, tumor border, and adjacent non-tumor samples, and GSE189175[25-27] with snRNA-seq data from liver biopsies of three MASLD-related HCC patients. Additional datasets for epigenetic modulation included RNA-seq from *KAT2A* knockout MASLD cells (GSE279791), TACC3 knockdown experiments in Panc-1 cells,[7] and RNA-seq of DLD1 colorectal cells following CRISPRCas9-mediated ZNF692 depletion (GSE215838).[28] For DNA methylation analysis, we utilized TCGA-LIHC Illumina 450K array data. To investigate the transcriptional and epigenetic consequences of DNMT1 loss, we analyzed CRISPR knockout RNA-seq data from K562 cells (GSE177511)[29] and H1-hESC cells (GSE170872),[29] along with our in-house liver-specific DNMT1 knockout datasets in mice, including transcriptomic (GSE67734) and methylomic (GSE67767) profiles.[30] To visualize the regulatory landscape of the *TACC3* locus, we used datasets from ENCODE for FOXM1 (ENCFF780EXO, ENCFF665DQA) and DNMT1 (ENCFF211ULJ, ENCFF361AJH) ChIP-seq, HepG2 ATAC-seq (ENCFF285FQS), and HepG2 CAGE (ENCFF205BRW, ENCFF683LBZ), as well as KAT2A ChIP-seq data (ENCFF853QRL, ENCFF490OJU) from HeLa-S3 cells.

Isoform switch analysis

Isoform switch analysis was performed using IsoformSwitchAnalyzeR 2.10.0,[31,32] with differential isoform usage assessed through DEXSeq[33,34] and SatuRn.[35] Functional

https://doi.org/10.3350/cmh.2025.1370

consequences of isoform-switching were evaluated using predicted changes in coding potential, protein structure, and subcellular localization. Significant isoform switches were identified using an absolute ΔIF cutoff of 0.1 and an FDR cutoff of 0.05. Venn diagrams were generated to show overlapping genes across different stages during HCC progression.

Single nucleus RNA sequencing (snRNA-seq)

snRNA-seq data were filtered to remove low-quality cells, mitochondrial genes, and doublets. Raw counts were normalized using Seurat's LogNormalize method, and highly variable features were selected for downstream analysis. Differential expression was performed using the FindMarkers function with a log2 fold-change threshold of 0.25 and adjusted *P*-value threshold.

Weighted gene co-expression network analysis (WGCNA)

WGCNA was performed on RNA-seq data, with differentially expressed genes (DEGs) identified using DESeq2.[36] Gene co-expression networks were constructed using a soft-thresholding power of 8; modules were identified by dynamic tree cutting (deepSplit=4, minimum module size=10), followed by module merging based on eigengene similarity (mergeCutHeight=0.07). Pathway enrichment analysis was performed on selected modules to identify functional roles in HCC progression.

High-dimensional WGCNA (hdWGCNA)

hdWGCNA was performed on snRNA-seq data using Seurat and the hdWGCNA framework. Cells were assigned to cell cycle phases (G1, S, G2/M) using Seurat's canonical gene sets. Genes expressed in ≥5% of cells were retained. To reduce sparsity, metacells were generated within each cell cycle phase using a k-nearest neighbor approach on the UMAP embedding (k=25, maximum shared cells=10), followed by log-normalization. Signed co-expression networks were constructed using soft-threshold power selection of 16 based on scale-free topology criteria; topological overlap matrices (TOMs) were computed using an unsigned method. Modules were identified by hierarchical clustering and dynamic tree cutting (minModuleSize=10, mergeCutHeight=0.07), module eigengenes were computed and harmonized across patients, and intramodular connectivity (kME) was used to define hub genes. Module activity was summarized at the single-cell level using UCell-based scoring.

Cell-cell communication analysis

Cell-cell communication was analyzed using CellPhoneDB[37] with single-cell RNA-seq data to identify ligand-receptor interactions between tumor and immune cells. Statistical significance was assessed using empirical shuffling, and the results were visualized using the CellChat database.[38]

10-fold cross-validation partial least squares (PLS) regression

PLS regression was applied to assess the relationship between transcription regulator (TR) expression and variability in *TACC3* and *KAT2A* isoform expression as well as switched genes. The dataset was divided into 10-fold cross-validation subsets, and R-squared values were used to quantify the variance explained by each TR.

DNMT1 knockout methylation analysis

DNMT1 knockout and tissue processing were performed as previously described.[30] Genome-wide DNA methylation in *Dnmt1* knockout and wild-type mouse livers was profiled using Illumina 450K arrays. Data were processed in R using the minfi package.[39] Probes for SNPs or non-autosomal chromosomes were filtered out, and data were normalized using preprocessFunnorm. Differential methylation analysis was performed with limma using a linear model that accounted for genotype, timepoint (4, 8, and 20 weeks), and their interaction. Key CpG sites for genes in the TACC3-KAT2A network (*Tacc3*, *Foxm1*, *Notch4*) were extracted for focused analysis and visualization.

ChIP-seq and chromatin accessibility data visualization

Publicly available ChIP-seq (FOXM1, DNMT1, KAT2A),

ATAC-seq, and CAGE-seq datasets in human HepG2 cells or primary liver tissue were obtained from ENCODE and GEO. BigWig signal tracks were imported and visualized over the TACC3 canonical transcript and promoter region (±2 kb from the transcription start site, hg38) using the Gviz package in R.

RESULTS

Isoform-switching is predominantly observed in tumor compared to adjacent non-tumoral tissue in HCC

HCC samples exhibit significantly elevated isoform diversity relative to matched non-tumoral tissues, indicating widespread AS and transcriptomic reprogramming during hepatocarcinogenesis (Fig. 1), emphasizing dynamic transcript entropy across liver disease progression to HCC (Supplementary Fig. 1).[40]

To characterize the AS dynamics of isoform-switching across liver disease stages, we analyzed significant isoform-level changes (dIF_{cutoff}=0.1; FDR correct isoform switch *P*-values <0.05) across five conditions (n=261 samples; healthy liver, MASLD, MASH, and matched HCC.NT, and HCC.T). The largest number of switches (75 genes) was observed during the transition from paired HCC.NT to HCC.T tissues (n=47 patients), followed by MASLD to HCC.NT transition, suggesting a disease-progressive transcriptome remodeling (Fig. 2A; Supplementary Table 1). Furthermore, a total of 22 isoform switched genes were enriched in liver-relevant cell types (HepG2, adipocytes) and spanned defined molecular functions related to metabolic homeostasis, signal transduction, and cellular stress responses across disease stages (Fig. 2B).

Since paired HCC.NT versus progressed HCC.T revealed the highest number of shared AS isoform-switching events compared to healthy liver to MASLD (Fig. 2A), this supports the notion that HCC.NT itself represents a molecular transition state within the disease progression. Although the liver parenchyma of MASLD-HCC patients often is non-cirrhotic (unlike alcohol- and viral-related HCCs), HCC.NT does not represent a static baseline. Instead, HCC.NT exhibits dynamic features that reflect both pre-tumor alterations and early tumor-like characteristics, which is supported by the high recurrence rates of 50–70% after 5 years post-resection compared to 10% for post-liver transplantation.[41] Thus, to minimize inter-patient variability and precisely capture the tumor-associated isoform changes, we focus our analysis on comparing the intra-patient HCC.NT versus HCC.T to dissect the AS isoform-level transcriptional reprogramming occurring during tumorigenesis.

The dominant AS events with biased usage in the tumor niches

To determine the dominant AS events in MASLD-HCC, we utilized our paired patient cohort to elucidate the progressive transcriptional changes. We identified in total 612 isoforms across 101 genes with significant isoform-switching and prioritized 111 isoforms (78 switches) across 67 genes based on predicted functional gene consequences (ΔIF≥0.1, Supplementary Table 1). The selected isoforms are primarily involved in promoting proliferation (*TACC3*, *MAPKAPK3*, *MAP2K1*), extracellular matrix remodeling (*ECM1*, *TNXB*), and inflammation (*IL1RAP, RCAN1*), progressing cancer (Supplementary Fig. 2A). Defined AS events revealed marked shifts in the transcriptional architecture, particularly involving alternative transcription start sites (ATSS) and termination sites (ATTS) (Fig. 2C) that, besides tumor progression, affect genes involved in metabolism and immune signaling. ATSS events showed a pronounced bias toward increased direct isoform usage in tumors alongside substantial contributions from exon skipping as well as alternative 3′ acceptor (A3) and 5′ donor (A5) site usage (Fig. 2D). These are patterns that may occur following mutational processes, from dysregulation of splicing factors and RNA-binding proteins[42] that lead to the inclusion or exclusion of functional domains, altering protein structure and affecting key tumorigenic processes.[43] Collectively, these findings underscore a tumor-promoting AS-enriched niche within the liver parenchyma of HCC.

Tumor-specific TACC3 isoform-switching decouples KAT2A-mediated chromatin regulation of NOTCH signaling

While isoform-switching is prevalent in HCC[2] (Fig. 2, Supplementary Table 1), the coordination of AS involved epigenetic regulation and the subsequent functional con-

https://doi.org/10.3350/cmh.2025.1370

Transcript diversity and complexity across liver disease categories.

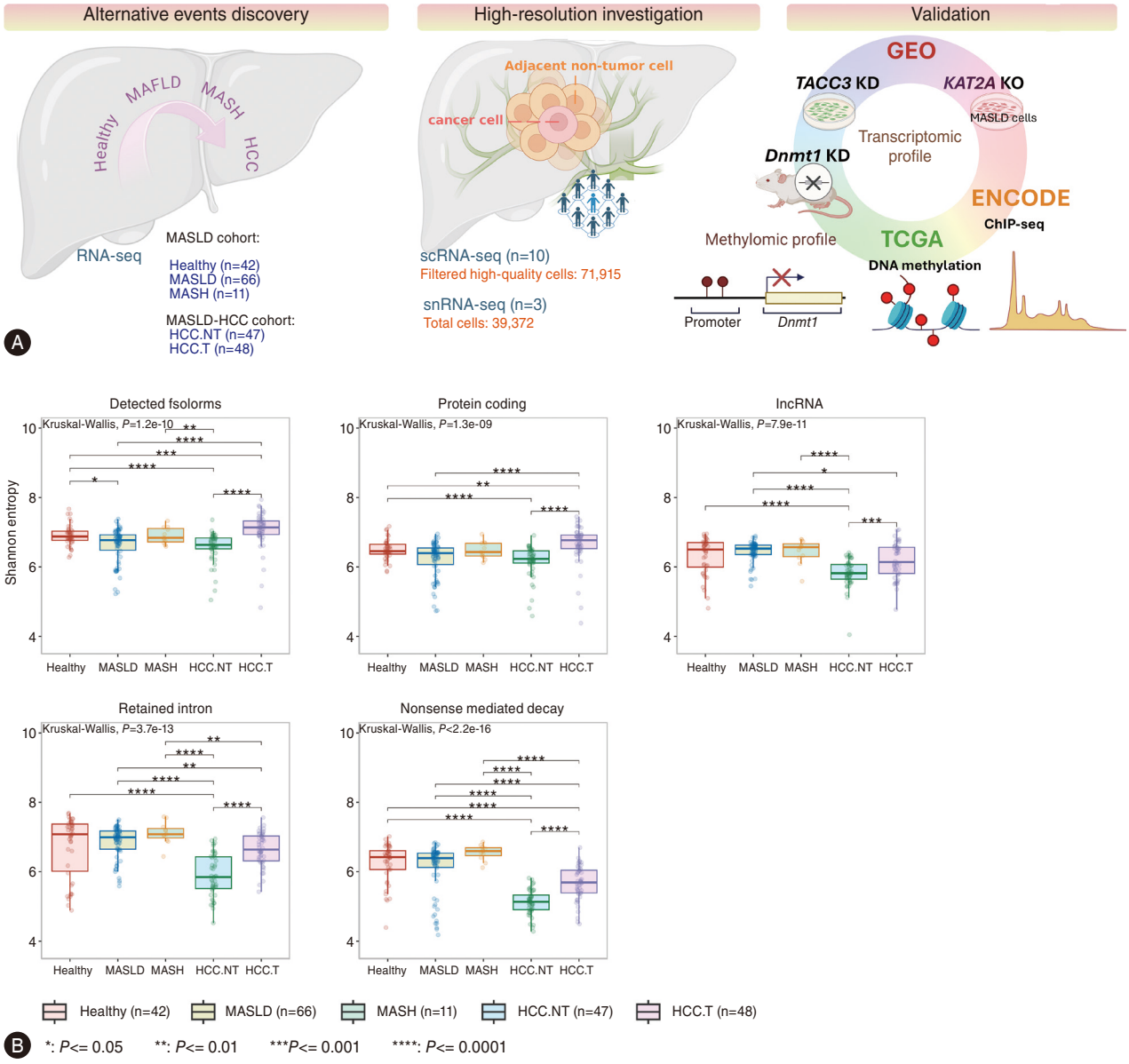

Figure 1. Transcript diversity across liver disease stages. (A) Schematic overview of the study. (B) Comparison of Shannon entropy across different disease stages (Healthy [n=42], MASLD [n=66], MASH [n=11], HCC.NT [n=47], and HCC.T [n=48]) for detected gene isoforms as well as protein-coding transcripts, lncRNAs, transcripts with retained introns, and transcripts susceptible to nonsense-mediated decay (NMD). Wilcoxon rank-sum tests were performed to assess differences among groups. HCC, hepatocellular carcinoma; HCC.NT, tumor-adjacent normal liver; HCC.T, tumor; MASLD, metabolic dysfunction-associated steatotic liver disease; MASH, metabolic dysfunction-associated steatohepatitis.

sequences remain challenging. In our analysis, TACC3 has emerged as an alternatively spliced gene whose isoform within the tumor exhibits epigenetic regulation by KAT2A (Supplementary Fig. 2). Exclusively, HCC tumors switch from a non-mediated decay (NMD)-sensitive isoform (TACC3-215) to the protein-coding alternative isoform (TACC3-201) (Fig. 3 and Supplementary Fig. 2C), which then couples to KAT2A.

This uniquely AS-regulated gene network is associated with the tumor microenvironment. Single-cell analysis revealed that the TACC3 expression peaks in tumor cells in G2/M-phase (Fig. 3D and Supplementary Fig. 3A–3C),

Isoform-switching and alternative splicing dynamics across liver disease progression.

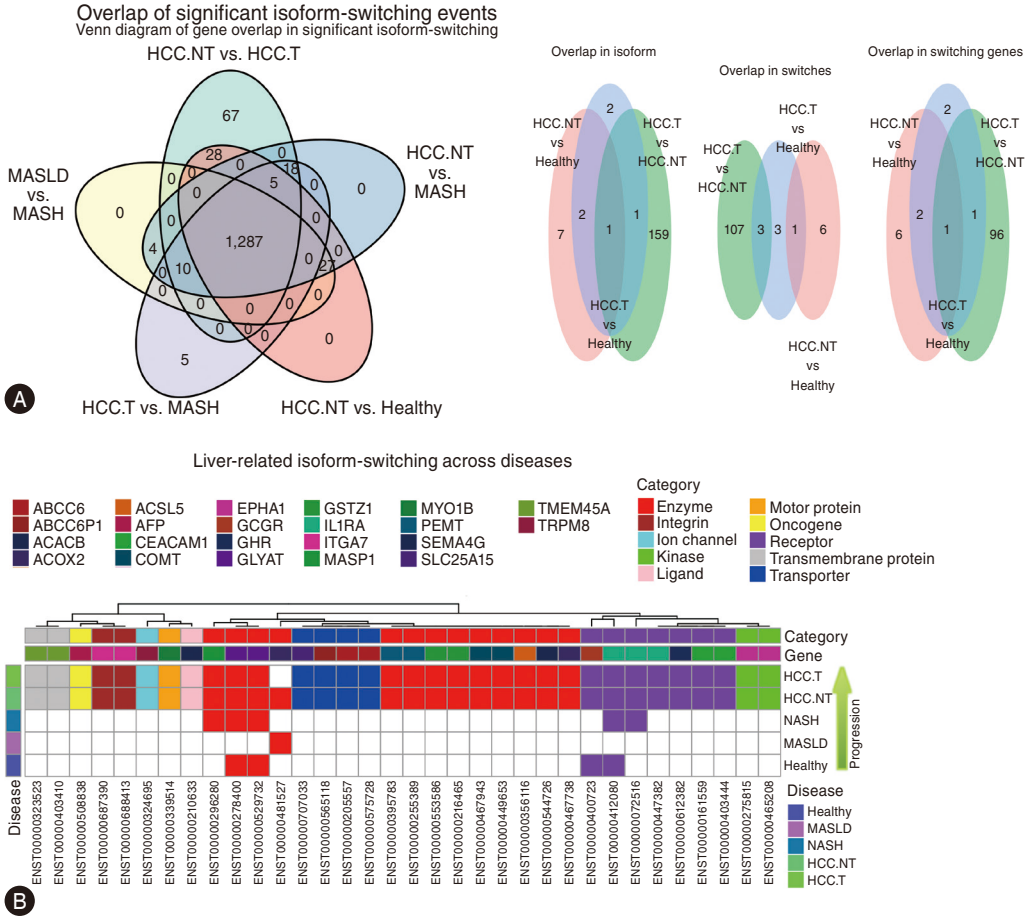

Figure 2. Alternative splicing dynamics and isoform-switching across liver disease progression. (A) Venn diagram illustrating the overlap of genes involved in significant isoform-switching. (B) Heatmap illustrating significant isoform switches in liver-enriched genes across disease stages, highlighting a predominant transition from HCC.NT to HCC.T. Rows represent disease groups ordered as Healthy, MASLD, MASH, HCC.NT, and HCC.T, while columns represent individual isoforms. (C) Plot showing the number of significant genes exhibiting AS isoform events in HCC.NT and HCC.T. The two plots distinguish splicing events with increased and decreased usage. A striped pattern indicates usage. (D) Splicing enrichment analysis of isoform switches in HCC.NT versus HCC.T samples. The plot illustrates the distribution of splicing events across various isoforms with a minimum of five events for significant isoforms (dIF_{cutoff} =0.1). A5, alternative 5' donor site (changes in the 5' end of the upstream exon); A3, alternative 3' acceptor site (changes in the 3' end of the downstream exon); AS, alternative splicing; ATSS, alternative transcription start site; ATTS, alternative transcription termination site; EI, exon inclusion; ES, exon skipping; HCC, hepatocellular carcinoma; HCC.NT, tumor-adjacent normal liver; HCC.T, tumor; IR, intron retention; MASLD, metabolic dysfunction-associated steatotic liver disease; MASH, metabolic dysfunction-associated steatohepatitis; MEE, mutually exclusive exon; MEI, multiple exon inclusion; MES, multiple exon skipping with >1 consecutive exon.

consistent with its known role in mitosis.[44] Beyond cell cycle regulation, our data emphasize that the isoform-switching from TACC3-215 to TACC3-201 mediates tumor-stroma-immune crosstalk by modulating the function of KAT2A, thereby promoting a chromatin-linked oncogenic reprogramming in the tumor (Fig. 3A). This restricted correlation of TACC3-201 with KAT2A in tumors (but not in the adjacent non-tumoral tissue) implies an isoform-dependent AS-driven epigenetic influence on the transcriptional state that may alter intercellular communication within the tumor niche.

We observed that TACC3 and KAT2A co-localized within a NOTCH4-associated co-expression module in premalignant tissues (Fig. 4A, Supplementary Fig. 4, Supplementary Fig. 5). In addition, GST pull-down assays confirm a direct interaction between TACC3 and KAT2A.[45] Both TACC3 and KAT2A are significantly elevated in tumor tissues compared with matched NT samples at both the mRNA and protein

https://doi.org/10.3350/cmh.2025.1370

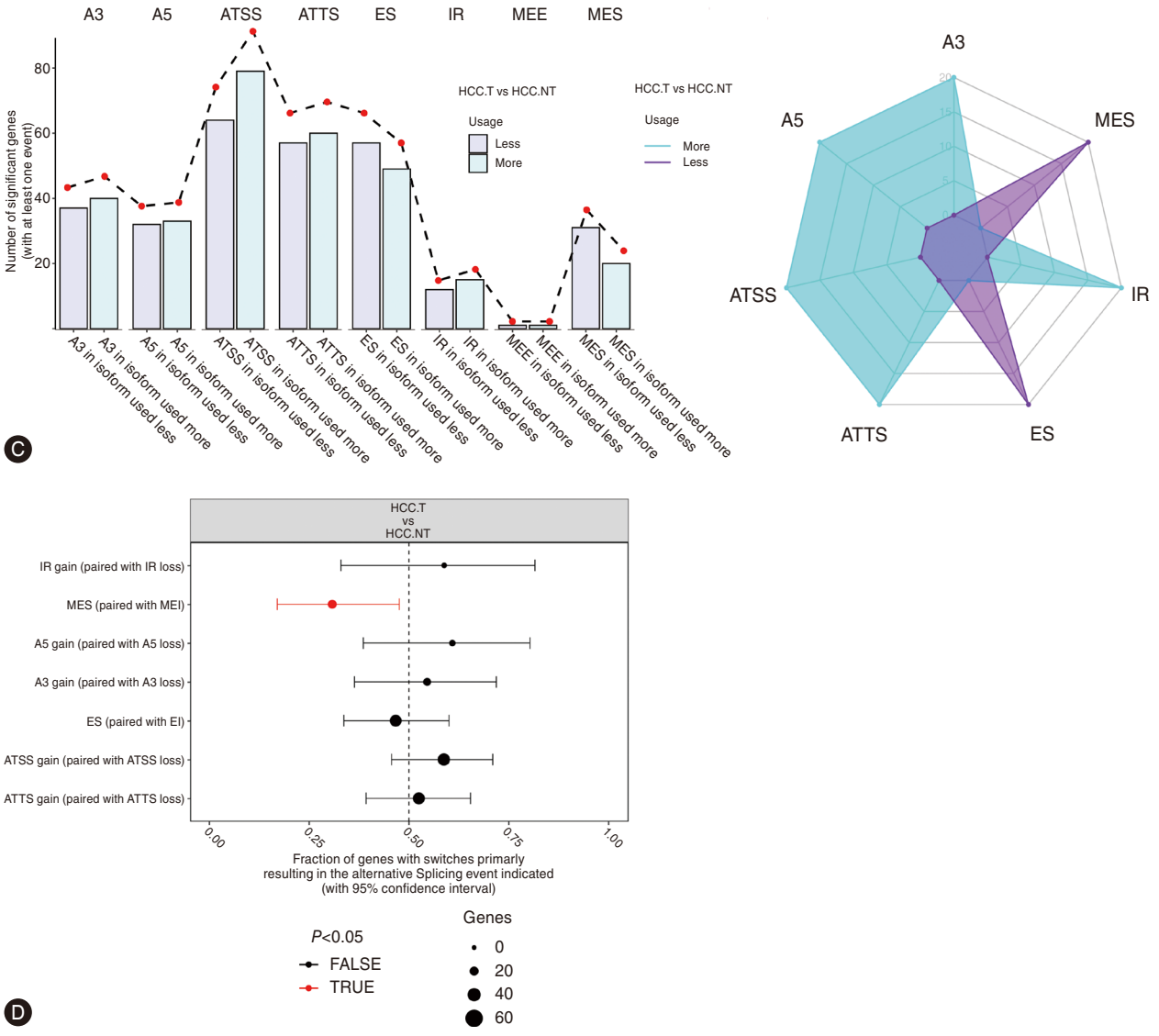

Figure 2. Continued.

levels (Fig. 4B, Supplementary Fig. 3F). However, this coordination in the premalignant tissues is context-dependent and undergoes tumor-specific modular reassignment despite strong preservation (Supplementary Fig. 3D, 3E), where TACC3 is shown to associate with genes involved in the mitotic regulation, chromatin remodeling, and DNA damage response (CDC20, AURKB, DNMT1, and H2AX), while KAT2A shifted to a distinct transcriptional hub (Fig. 4A) enriched for genes involved in DNA repair (*MUS81*, *PIDD1*), signal transduction (*HRAS*, *ARFGAP1*), RNA processing and translation regulation (*PABPC1L*, *SAMD4B*, *TRMU*, *NSUN5P2*), and chromatin organization (*PRR14*, *ZNF692*). This segregation coincided with the tumor-specific loss of the coupling between TACC3-201 and NOTCH4 (Fig. 4C, 4D), suggesting a unique AS-driven rewiring of the NOTCH regulatory axis.

KAT2A orchestrates NOTCH signaling with TACC3 as a context-dependent modulator

While activation of NOTCH signaling in the liver has been shown to promote cholangiocarcinoma through hepatocytic transdifferentiation in transgenic models,[46] our data indicate that in MASLD-HCC, this axis undergoes selective

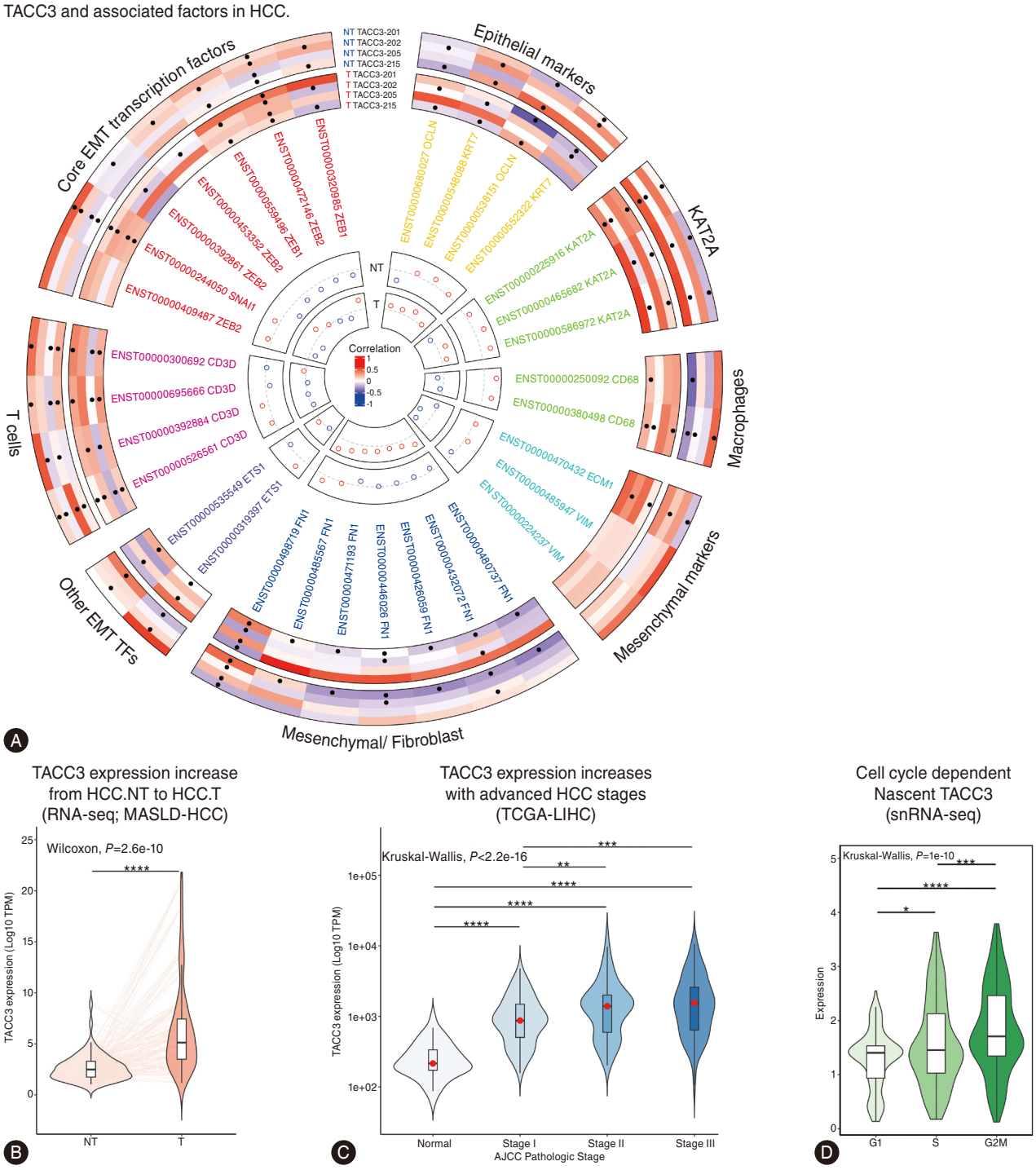

Figure 3. Correlation patterns, expression, and pathway analyses of TACC3 and associated factors in HCC. (A) Circular heatmap visualization of nonparametric correlation patterns across different conditions. Heatmaps represent the correlation of the TACC3 isoform with KAT2A, cell type markers, and EMT markers in non-tumor (NT) (outer circle) and tumor (T) (inner circle). Significant differences are presented by black dots whereas row-wise standard deviations are given by innermost red/blue circles. (B) *TACC3* expression in HCCs and non-tumoral tissues (MASLD-HCC cohort). (C) *TACC3* expression from normal and across HCC tumor AJCC stages (TCGA-LIHC). (D) Violin and box plots showing cell cycle (G1, S, and G2/M) phase-dependent nascent expression of *TACC3* in single-nucleus RNA sequencing data. Statistical significance was assessed using Wilcoxon test. AJCC, American Joint Committee on Cancer; EMT, epithelial-mesenchymal transition; HCC, hepatocellular carcinoma; HCC.NT, tumor-adjacent normal liver; HCC.T, tumor; MASLD, metabolic dysfunction-associated steatotic liver disease; MASH, metabolic dysfunction-associated steatohepatitis.

https://doi.org/10.3350/cmh.2025.1370

TACC3-KAT2A regulatory landscape.

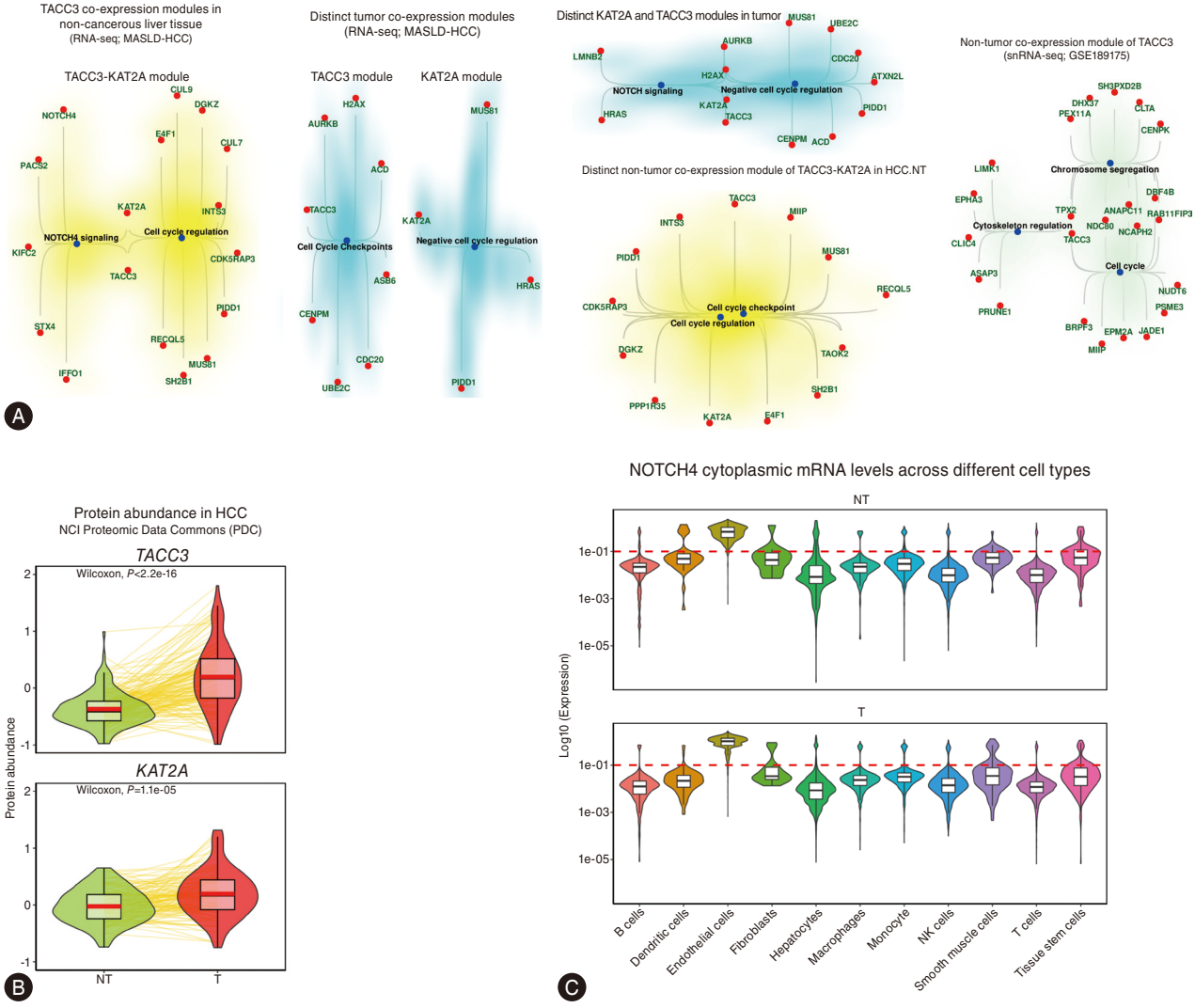

Figure 4. TACC3-KAT2A regulatory interactions. (A) TACC3-KAT2A pathway and module networks. (B) Paired protein abundance of TACC3 and KAT2A in HCC tumors (T) and matched adjacent normal tissues (NT). Data are from the NCI Proteomic Data Commons (PDC). Lines connect paired samples from the same patient, with red bars indicating the mean. (C) NOTCH4 is enriched in endothelial cells. (D) Significant correlation is observed between *TACC3* isoforms and KAT2A and NOTCH4. (E) Heatmap showing the association between TACC3, KAT2A, and NOTCH4 as well as ENCODE-enriched histone modifications. (F) *TACC3* and *NOTCH4* expression levels in wild-type (WT) and *KAT2A* knockout (KO). HCC, hepatocellular carcinoma; HCC.NT, tumor-adjacent normal liver; HCC.T, tumor; MASLD, metabolic dysfunction-associated steatotic liver disease.

modulation rather than full activation. Specifically, KAT2A appears to orchestrate NOTCH signaling in tumors, while TACC3 functions as a context-dependent modulator of NOTCH (Fig. 5A).

In MASLD-HCC,[47] we have observed a significant dysregulation of the NOTCH pathway between paired tumor and non-tumoral samples (Fig. 5A). Functional validation of this regulatory network was confirmed in the *KAT2A* liver-specific knockout, emphasizing the repressive role of KAT2A. KAT2A liver deletion showed upregulation of *TACC3*, *NOTCH4*, and canonical NOTCH signaling (Figs. 4F, 5B, Supplementary Fig. 4D). In contrast, TACC3 knockdown did not significantly alter NOTCH signaling genes (Fig. 5C), specifying KAT2A as the upstream regulator in this axis. Mechanistically, KAT2A modulates TACC3 and NOTCH-related genes via coordination of H3K4me1 and H3K9ac, and

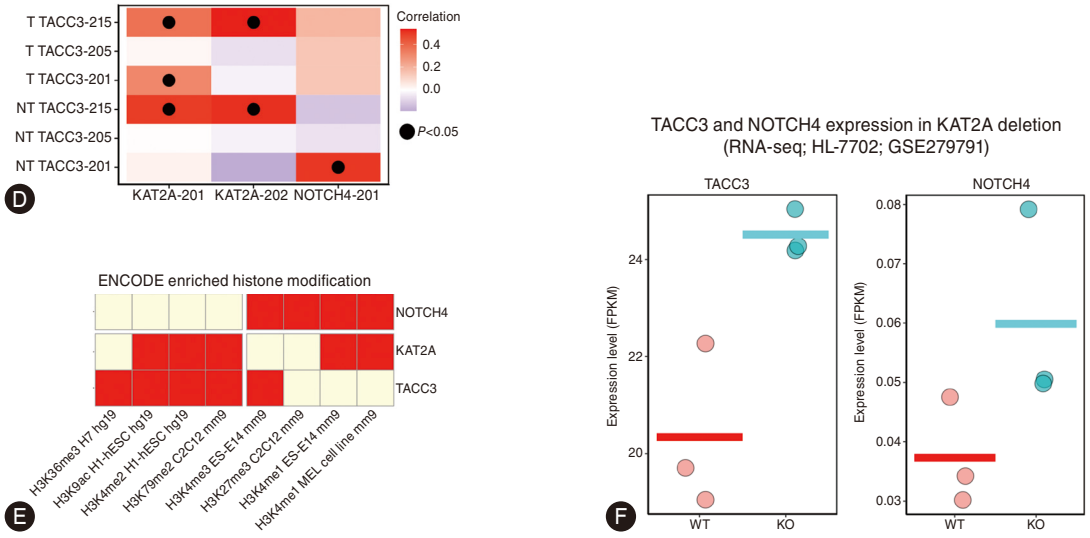

Figure 4. Continued.

recruitment of downstream NOTCH-responsive regulatory elements (Fig. 4E, Supplementary Fig. 6A–6C). While TACC3 is upregulated in many cancers and selectively binds the NOTCH4 intracellular domain, these results show that TACC3 is not the main driver of NOTCH signaling, but rather acts as a context-dependent co-regulator that fine-tunes the pathway activity downstream of KAT2A.

Transcriptomic profiling revealed that KAT2A and TACC3 exhibit both synergistic and divergent effects (Fig. 4A). TACC3 knockdown altered a subset of KAT2A target genes, whereas KAT2A loss induced broader transcriptional changes, implicating genes involved in cell cycle progression, DNA repair, and chromatin organization (Fig. 5D). Coordinated TACC3 and KAT2A expression levels shift within coregulated gene sets included pathways tied to nuclear transport, metabolism, and DNA damage response, with some targets showing opposing regulation between KAT2A deletion and TACC3 knockdown (Fig. 5E).

Further analysis revealed that the regulatory impact of TACC3 is tissue- and context-dependent (Fig. 6A, 6B). TACC3 knockdown disrupted mitotic regulation in tumor cells and recombinational DNA repair in non-malignant tissues (Fig. 6A–6C, Supplementary Fig. 5), indicating its dual role in supporting proliferation during malignancy while maintaining genomic integrity in non-tumoral tissues. Notably, this included downregulation of genes critical for chromosome segregation, replication, and mitochondrial metabolism, along with upregulation of pro-apoptotic BBC3/PUMA, implicating TACC3 in promoting tumor cell survival via p53-mediated apoptosis (Supplementary Fig. 6A–6D).

TACC3 also modulates the chromatin architecture by regulating key epigenetic factors. Knockdown of TACC3 directly reduced KAT2A expression and repressed additional chromatin modifiers (EZH2, KDM1A, and HDAC4), while upregulating KDM4A, HDAC6, and CBX7 (Supplementary Fig. 6E). These findings position TACC3 as a transcriptional modulator that indirectly controls chromatin states through epigenetic enzymes, while also influencing the expression of KAT2A itself, suggesting a potential autoregulation within the chromatin landscape. Such feedback loop may help stabilize transcriptional outputs during tumor progression, extending the influence of TACC3 beyond the NOTCH pathway to a broader control of transcriptional programs. This addresses the potential role of EZH2/PRC2 regulation, as our data support KAT2A as the primary upstream effector, with TACC3 contributing to chromatin feedback and fine-tuning, rather than by itself serving as a dominant regulator of NOTCH activation. These data define KAT2A as centrally positioned within NOTCH signaling and chromatin homeostasis with TACC3 functioning as the context-specific effector that adjusts the transcriptional programs (cell cycle control and apoptotic balance) in HCC.

https://doi.org/10.3350/cmh.2025.1370

Dysregulation and transcriptional impact of Notch signaling.

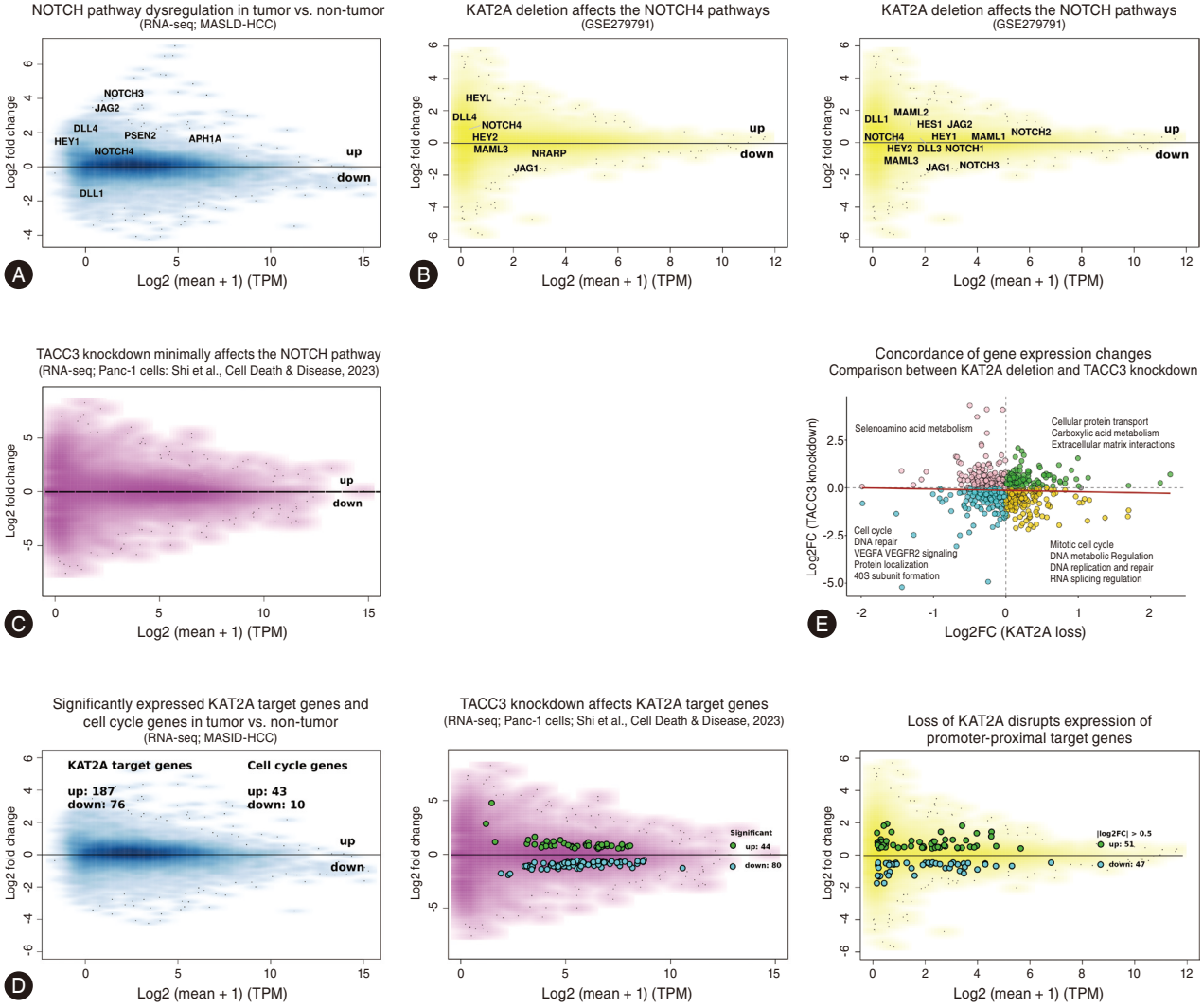

Figure 5. Dysregulation and transcriptional impact of Notch signaling in MASLD-HCC. (A) Differential expression of Notch pathway genes in MASLD HCC.NT versus HCC.T. (B) Differential expression of Notch4 and Notch pathway genes in *KAT2A* deletion (GSE279791). (C) Differential expression of Notch pathway genes in *TACC3* knockdown. (D) Left: the number of KAT2A target genes and cell cycle-related genes that are significantly differentially expressed between HCC.T and HCC.NT samples. Middle: the number of KAT2A target genes affected upon *TACC3* knockdown. Right: Loss of KAT2A disrupts the expression of promoter-proximal KAT2A target genes. (E) Concordant gene expression changes and enriched pathways observed between *KAT2A* deletion and *TACC3* knockdown. HCC, hepatocellular carcinoma; HCC.NT, tumor-adjacent normal liver; HCC.T, tumor; MASLD, metabolic dysfunction-associated steatotic liver disease.

Transcriptional rewiring of the TACC3-KAT2A network in tumor progression

To investigate the disruption of the TACC3-KAT2A regulatory network during the transition from non-cancerous tissues to HCC, and the major driving force to separate their co-expression module, we applied a transcription factor enrichment analysis to prioritize the top 30 TRs predicted to regulate *KAT2A*, *TACC3*, or both. Several TRs exhibited significant upregulation in HCC compared to non-tumor tissues (Fig. 6D). Notably, *E2F1* and *MYBL2*, which are predicted to co-regulate both *TACC3* and *KAT2A*, were among the most upregulated factors ($log_2FC>3$), suggesting their involvement in driving the concurrent augmented expression of these genes and establishing oncogenic transcriptional programs.[48] Additionally, *FOXM1*, *MYBL1*,

Pathway overlap and transcriptional regulation associated with TACC3 and KAT2A in liver tissues.

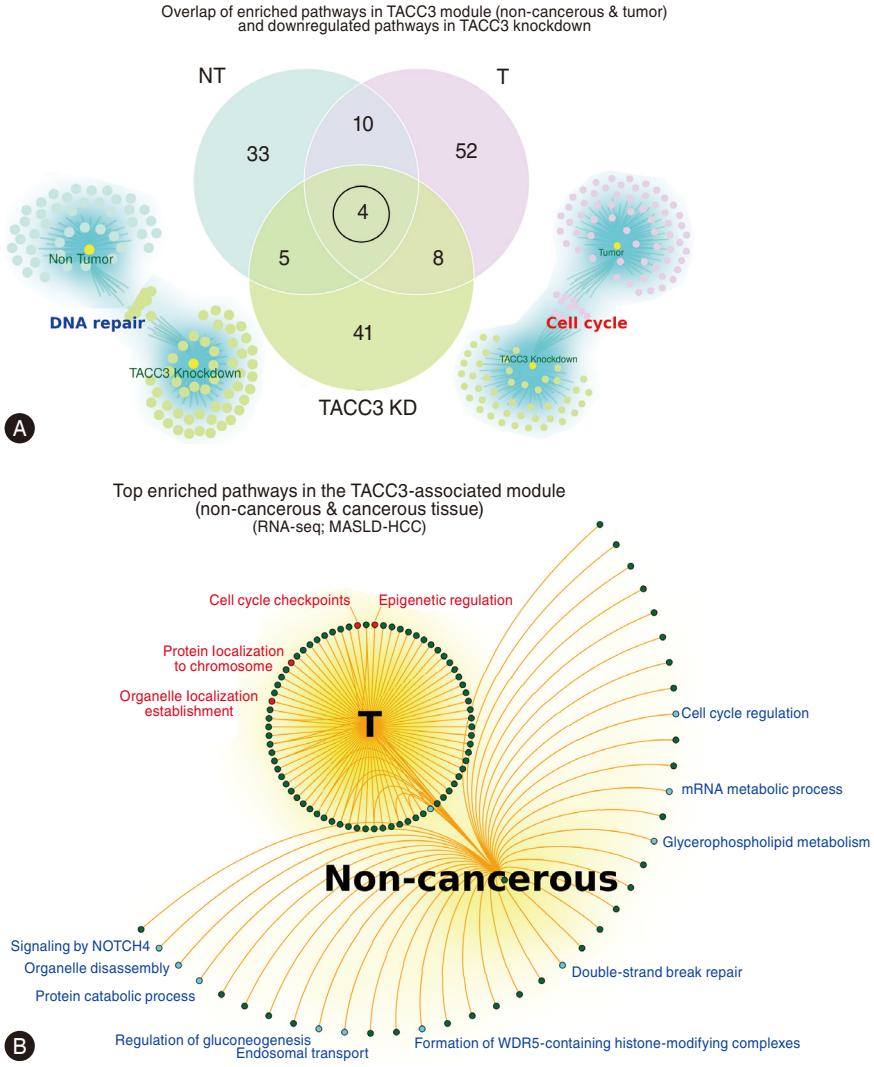

Figure 6. Integrated analysis of TACC3-related pathways. (A) Overlap of enriched pathways among *TACC3* co-expression modules in non-tumor, tumor, and *TACC3* knockdown (KD) conditions. (B) Network graph of enriched biological processes in HCC.NT and HCC.T tissues. (C) Venn diagram illustrating the overlap of the top 50 transcription factors (ChEA3) identified in WGCNA modules associated with TACC3-KAT2A, TACC3, and KAT2A in HCC.NT and HCC.T tissues. (D) Differential expression of top transcriptional regulators (TRs) associated with TACC3, KAT2A, or both between HCC.T and HCC.NT tissues. (E) Density plots showing the proportion of *TACC3* and *KAT2A* expression variance explained by FOXM1 and ZNF692. HCC, hepatocellular carcinoma; HCC.NT, tumor-adjacent normal liver; HCC.T, tumor; MASLD, metabolic dysfunction-associated steatotic liver disease; WGCNA, weighted gene co-expression network analysis.

TIGD3, *CBX2*, and *GMEB2*, which selectively are associated with *TACC3*, also showed marked upregulation in HCC, a trend independently validated in TCGA-LIHC data. This tumor-specific enrichment supports a model, in which *TACC3* becomes transcriptionally uncoupled from *KAT2A* and engages a distinct set of TRs that reinforce its elevated expression. To investigate whether *FOXM1* (or other tumor-enriched TRs) drives remodeling of the *TACC3* transcriptional co-expression modules[49] and contributes to the uncoupling of the TACC3-KAT2A regulatory module in HCC, we applied PLS regression analysis to assess to what degree variances observed in *TACC3* and *KAT2A* expression levels may be explained by FOXM1. We showed that the TACC3-201 isoform (rather than TACC3-215) is explained by FOXM1, while *KAT2A* expression is primarily explained by another TR (ZNF692) (Fig. 6E, Supplementary Fig. 7A, 7B). This is consistent with CRISPR-Cas9-mediated knockout of *ZNF692* observed in DLD1 colorectal cells, which led to

https://doi.org/10.3350/cmh.2025.1370

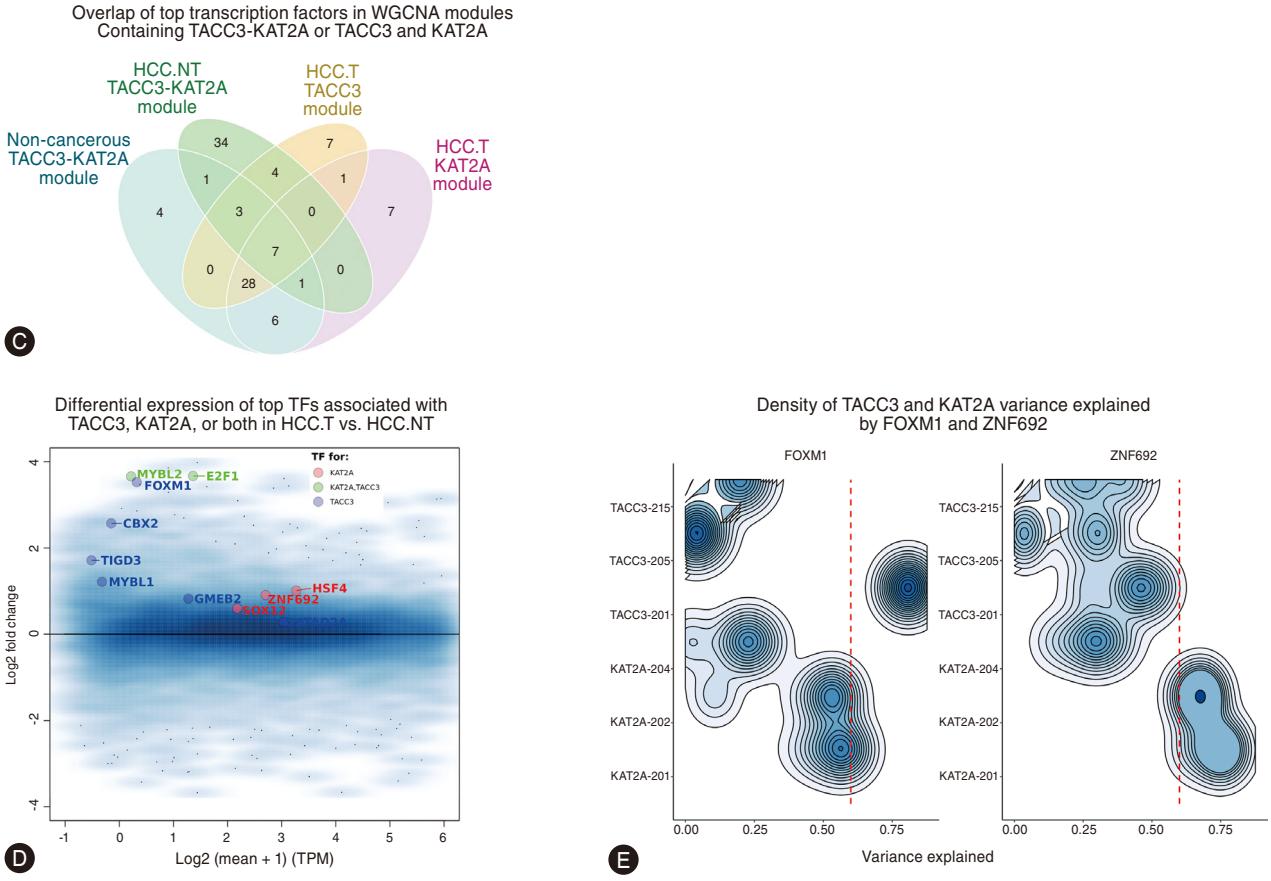

Figure 6. Continued.

a coordinated upregulation of both *KAT2A* and *TACC3* (Supplementary Fig. 7C) supporting a repressive role for ZNF692 in the pre-malignant regulatory state and highlighting its potential role in maintaining the integrity of the TACC3-KAT2A transcriptional module. As such, *FOXM1* and *ZNF692* execute distinct but complementary roles in shaping *TACC3* and *KAT2A,* contributing to the uncoupling of their transcriptional regulation during tumorigenesis. To expand on the role of *FOXM1* in broader transcriptional reprogramming, we next examined its involvement, alongside other key TRs, in the context of HCC isoform-switching.

DNMT1 is a key transcriptional regulator associated with isoform switched genes

Among the main TRs enriched for the 67 switched genes (Supplementary Table 1), several (*DNMT1*, *FOXM1*, *ETV7*, *E2F1*, *MYCL*, *CREB3L1*, *E2F4*, *TCF21*, *MYBL2*, and *HNF4)* showed a cumulative increase in the number of associated genes (Supplementary Fig. 7D). These TRs exhibit significant differential expression between HCC.T and HCC.NT tissues and further were validated in TCGA-LIHC. Notably, *DNMT1*, *FOXM1*, *ETV7*, and *E2F1* alone account for 49% of the switched gene regulation (Fig. 7A).

PLS modeling with 10-fold cross-validation demonstrated that *DNMT1* alone accounts for 80% of the variance in a total of 47 out of 67 switched genes (Fig. 7B). In contrast, *FOXM1* predominantly influences isoform-switching in genes such as *TACC3*, *PTTG1*, and *PKMYT1*, while *ETV7* has minimal impact on the isoform variance (Supplementary Fig. 7E). Overall, DNMT1 plays a dominant role in regulating AS, whereas the effects by *FOXM1* is minor within this context.

Most isoforms are protein-coding (44 out of 67) and explain >80% of the variance caused by *DNMT1.* This is followed by isoforms with undefined CDS, retained introns, and few lncRNAs as well as NMD-mediated isoforms (Supplementary Fig. 7F). This prevalence in protein-coding isoforms suggests that DNMT1 may play a significant role

Dnmt1-driven transcriptional and epigenetic alterations in MASLD-HCC.

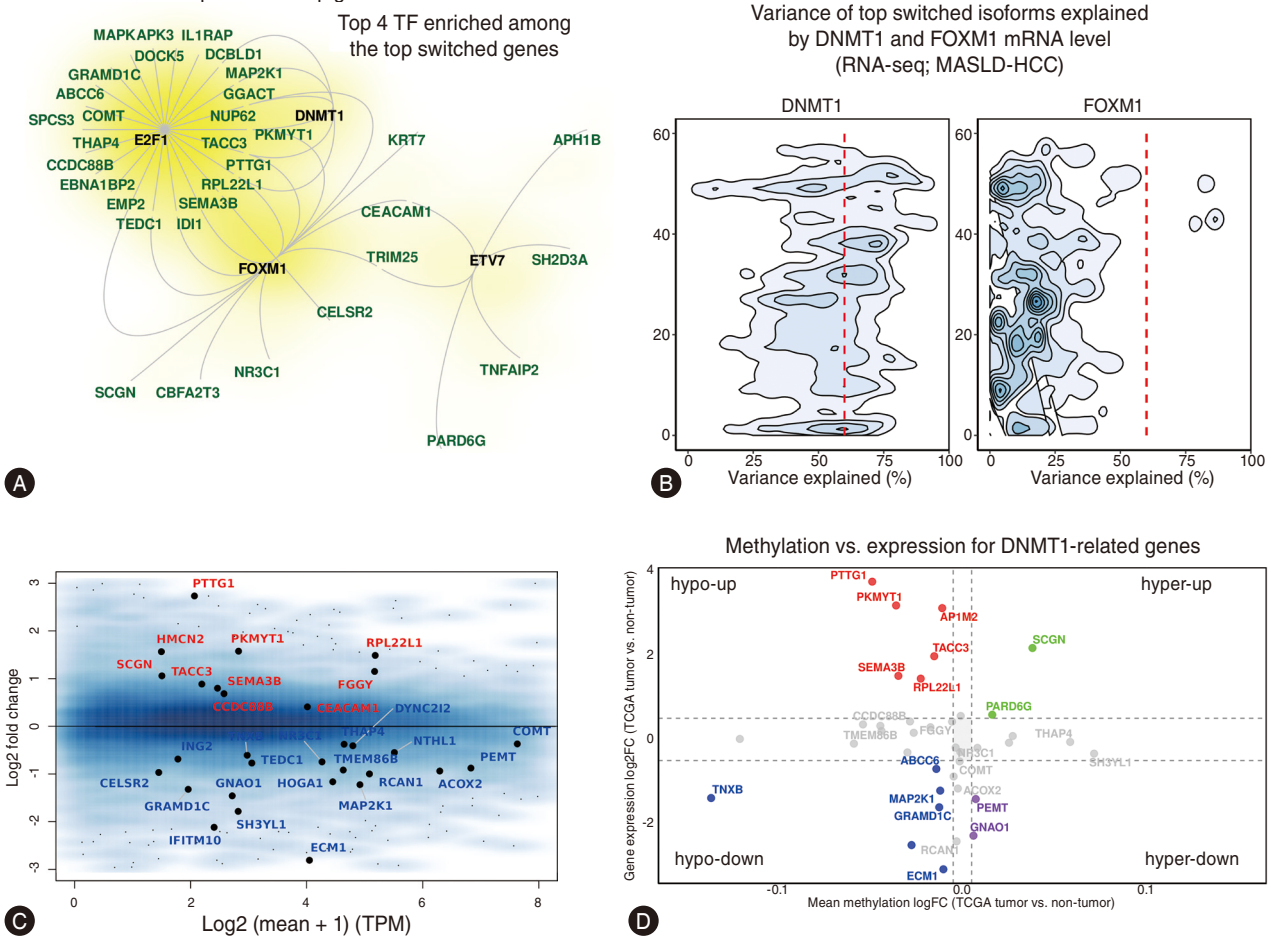

Figure 7. DNMT1 and FOXM1 activity explain isoform variance in MASLD-HCC. (A) Network visualization of transcription factors (TF) and associated genes among switched genes. Nodes represent TFs and genes, with edges connecting each TF to its overlapping genes. (B) Variance of top switched genes explained by DNMT1 and FOXM1 activity. Contour lines represent density estimates of the variance distributions. Threshold is represented by red dashed line explaining 60% of the variance. (C) Scatterplot showing all differentially expressed genes (DEGs) plotted by $\log_2$ mean expression levels versus $\log_2$FC(HCC.T vs. HCC.NT) in MASLD-HCC. Labeled DNMT1-regulated genes with isoform variance (R^2>0.8) and concordant expression changes validated in TCGA-LIHC. Upregulated genes (red), and downregulated genes (blue) in tumors. (D) Relationship between differential methylation and gene expression changes in DNMT1-regulated genes. Scatterplot displaying tumor and non-tumor (TCGA-LIHC) mean methylation (logFC) versus gene expression ($\log_2$FC). Labeled genes highlight concordance observed in MASLD-HCC. HCC, hepatocellular carcinoma; HCC.NT, tumor-adjacent normal liver; HCC.T, tumor; MASLD, metabolic dysfunction-associated steatotic liver disease.

in suppressing the expression of 20 functional genes involved in glycerolipid, carboxylic acid, and oxytocin signaling pathways. Genes that show concordant expression patterns with the TCGA dataset are labeled in Figure 7C.

As DNMT1-FOXM1 predominantly controls the observed isoform variance in tumors, their crosstalk governs context-dependent epigenetic regulation. As such, *DNMT1* is broadly overexpressed in HCC and drives context-dependent methylation changes. While targets such as *PEMT*, *GNAO1* show typical silencing by hypermethylation, TACC3 exhibits promoter hypomethylation and increased expression (Figs. 7D, 8A). This paradoxical regulation is resolved by *FOXM1*, which is bound to hypomethylated open DNA regions at the *TACC3* locus (Fig. 8B, Supplementary Fig. 8A). FOXM1 binds near the TACC3-201 promoter enhancing its transcription, while hypomethylation near the TACC3-215 transcription start site independently may drive NMD-sensitive transcript expression in tumors.

To directly examine the potential spatial interplay of these key regulators at the *TACC3* locus, we visualized public ENCODE ChIP-seq data across multiple cellular contexts. In HepG2 cells, we observed a striking co-occupancy

https://doi.org/10.3350/cmh.2025.1370

Epigenetic and transcriptional regulation of TACC3.

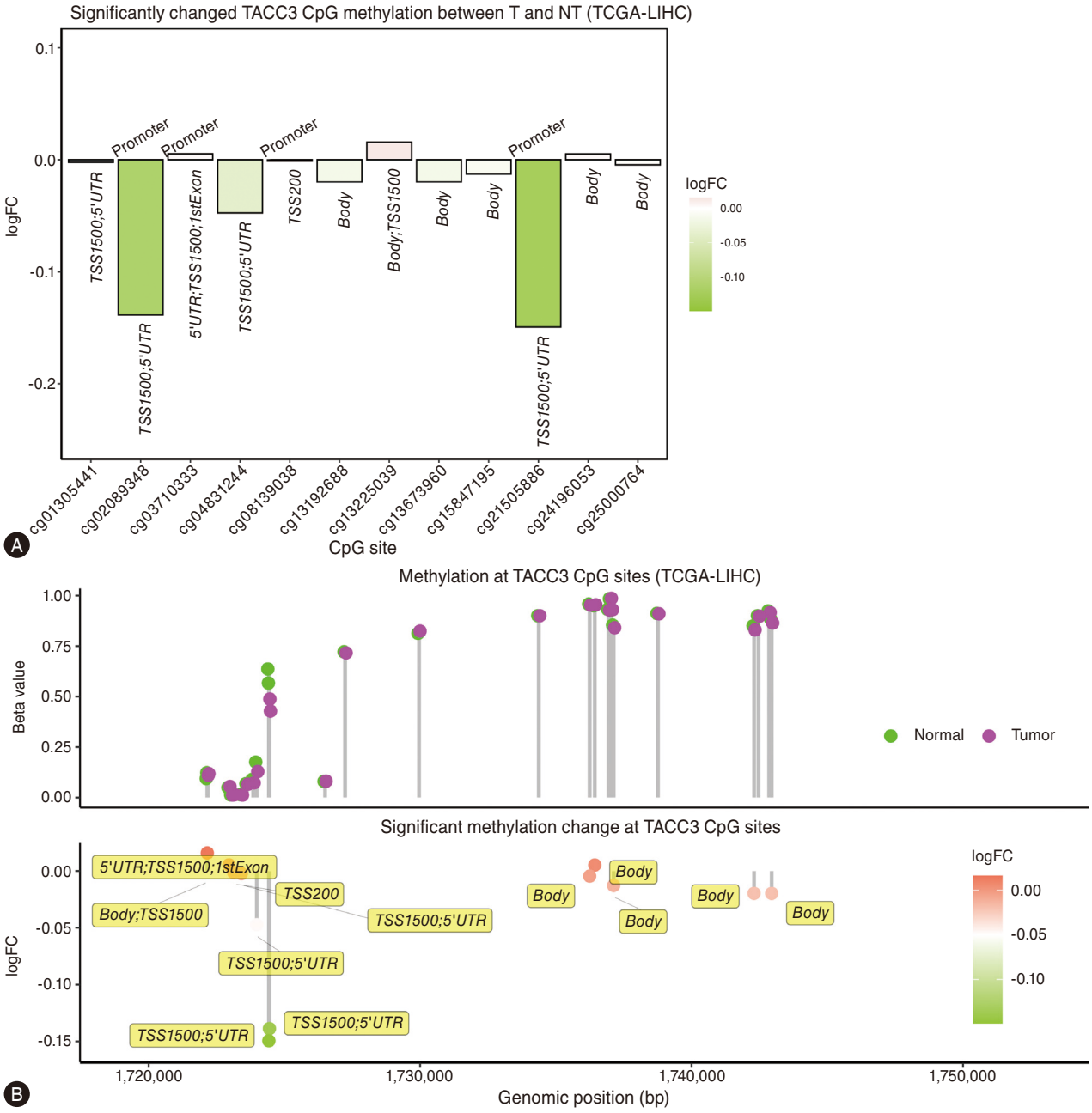

Figure 8. Epigenetic and transcriptional regulation of TACC3**.** (A) Bar plot illustrating the significant methylation logFC changes at various CpG sites within the *TACC3* gene. (B) DNA methylation and FOXM1 ChIP-seq signals (hg19) across the *TACC3* promoter region. Top: Lollipop plot showing CpG sites associated with *TACC3*. X-axis shows genomic positions; Y-axis indicates β values. Bottom: Differential methylation at significant CpG sites near *TACC3*. Only CpG loci with adjusted *P*-value<0.05 are shown. Vertical segments represent the logFC (tumor vs. normal) methylation levels. Labels denote annotated gene regions based on UCSC annotations. It is shown in hg19 to match the methylation array annotation. (C) Genome browser tracks of public ENCODE ChIP-seq data across the canonical TACC3-201 gene body and promoter region (chr4:1,719,521-1,744,171, hg38). Tracks show: (i) FOXM1 binding signal and fold-change over input, (ii) DNMT1 binding signal and fold-change, (iii) KAT2A binding signal and fold change, (iv) HepG2 ATAC-seq signal, and (v) HepG2 CAGE signal (transcription start site activity). A prominent FOXM1 binding peak overlaps the TACC3 promoter region, which also shows DNMT1 and KAT2A occupancy in ENCODE datasets, together with active chromatin features and activated transcription starting site. It uses hg38 to align with ENCODE datasets. (D) ATAC-seq signal across the TACC3 locus in human hepatocytes (GSE298820). Chromatin accessibility is reduced upon FOXM1 inhibition compared with control (blue: control, orange: FOXM1 inhibition), highlighting FOXM1's potential role in maintaining open chromatin at the TACC3 locus.

 https://doi.org/10.3350/cmh.2025.1370

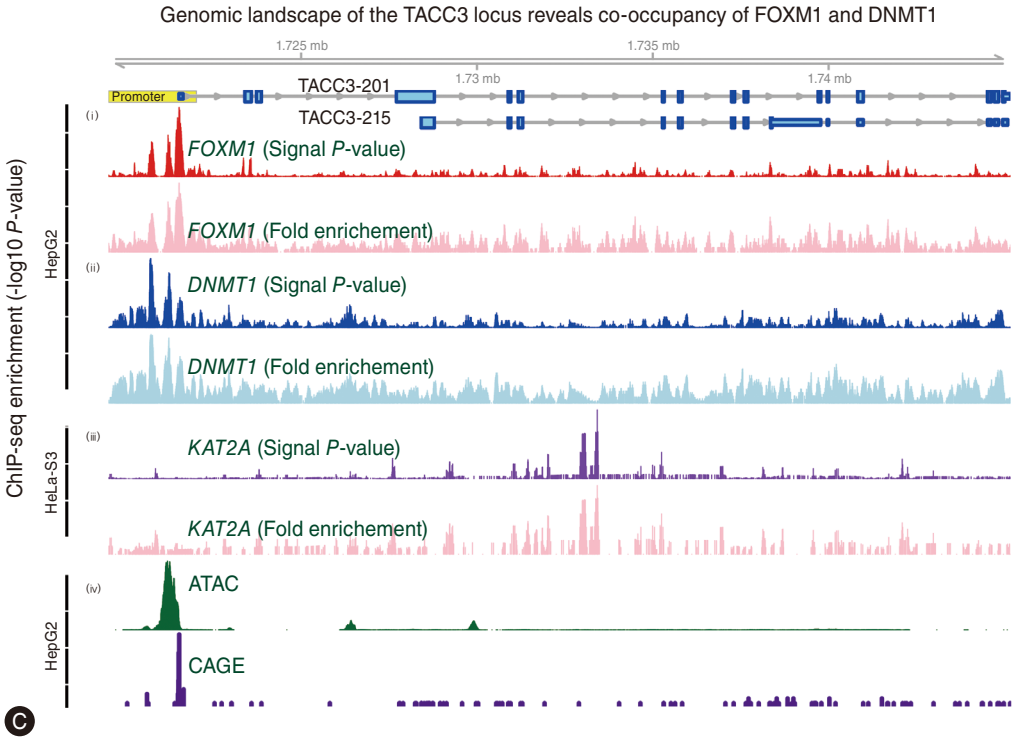

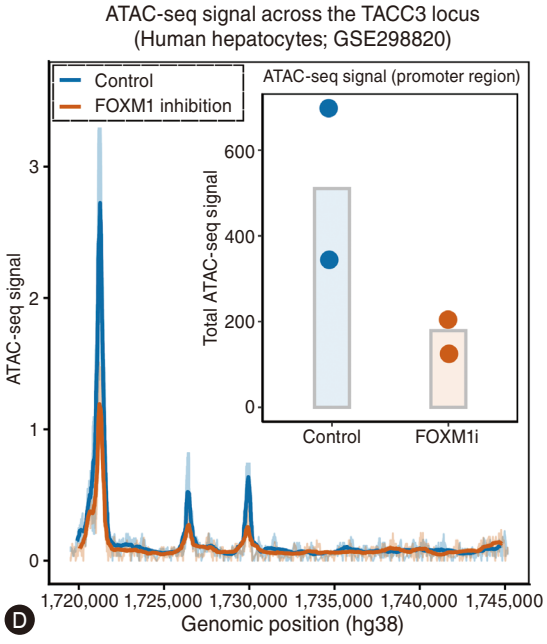

Figure 8. Continued.

where binding peaks for FOXM1 and DNMT1 converged directly over the active *TACC3-201* promoter region, precisely within a zone of open chromatin defined by ATAC-seq and active transcription marked by CAGE signals (Fig. 8C).

Dnmt1 loss uncouples the *Foxm1-Tacc3* regulatory axis via locus-specific epigenetic remodeling in mice

Although Foxm1 is a known transcriptional activator of

https://doi.org/10.3350/cmh.2025.1370

Tacc3,[21] and FOXM1 inhibition reduces chromatin accessibility at the TACC3 promoter (Fig. 8D), analysis of liver-specific *Dnmt1* knockout mice[30] reveals a disruption of the Foxm1-Tacc3 regulatory axis. Specifically, *Dnmt1* loss is associated with a dissociation between *Foxm1* upregulation and *Tacc3* downregulation (Supplementary Fig. 8A), indicating that *Tacc3* expression is constrained by additional epigenetic or post-transcriptional mechanisms in this context.

Consistent with this interpretation, we previously showed that KAT2A-mediated histone acetylation coordinates TACC3 transcriptional regulation (Fig. 4F). Moreover, DNMT1 ChIP-seq data demonstrate direct DNMT1 occupancy near the *Tacc3* locus (Fig. 8C, Supplementary Fig. 8B), positioning DNMT1 as a locus-specific regulator of *Tacc3* expression. Notably, *Dnmt1* loss induces a strong positive correlation between *Tacc3* and *Foxm1* expression (ρ=0.61, P=0.06), a relationship absent in wild-type controls (ρ=0.09, P=0.9) (Supplementary Fig. 8A). This shift suggests that DNMT1 normally restrains FOXM1-dependent activation of *Tacc3*, and that its removal unmasks a latent transcriptional dependency.

DISCUSSION

Our study reveals a novel mechanism by which HCC progression is driven through disruption of the TACC3-KAT2A-NOTCH4 axis and FOXM1-mediated insulation of *TACC3* from DNMT1 silencing. In premalignant tissues, TACC3 and KAT2A are co-regulated, supporting a functional interaction entwined to chromatin remodeling. This association is lost in HCC tumors, where their correlation re-emerges at the gene level, suggesting a shift in regulatory dynamics during tumorigenesis. While FOXM1 is associated with the *TACC3* locus, our study does not suggest that FOXM1 directly recruits KAT2A. Instead, TACC3 through its transforming acidic coiled-coil domain may scaffold KAT2A to chromatin, creating a permissive environment for coordinated transcriptional and splicing regulation. Further structural and protein-protein studies will be required to definitively confirm this interaction.

Although *DNMT1* is broadly upregulated in HCC, its activity appears to be locus specific. At the *TACC3* locus, we observe DNA hypomethylation and increased expression, suggesting an escape from DNMT1-mediated repression. This paradoxical regulation is resolved by FOXM1, a transcription factor known to engage co-activators, such as KAT2A. Matched ChIP-seq and methylation datasets reveal that FOXM1 binding peaks coincide with hypomethylated regions enriched for active chromatin mark H3K27ac, implicating FOXM1 as a chromatin-level activator that safeguards genes like TACC3 from epigenetic silencing.

These data support a model in which FOXM1 creates a permissive chromatin state at the *TACC3* promoter, insulating it from DNMT1 activity. This coordinated regulation permits sustained TACC3 expression despite the global upregulation of a repressive epigenetic machinery in HCC. Thus, TACC3 is located at the intersection of transcriptional activation, chromatin remodeling, and isoform-specific splicing, representing a critical effector of AS oncogenic reprogramming in HCC. However, these DNMT1-dependent effects should be interpreted as supportive and context-dependent, given the potential for long-term epigenetic consequences of DNMT1 knockout.

The loss of KAT2A-TACC3 interaction alters downstream signaling pathways, notably of NOTCH4 signaling. In non-tumoral contexts, KAT2A may suppress NOTCH4 signaling by recruiting repressive chromatin modifiers. However, upon KAT2A depletion or its functional uncoupling from TACC3, NOTCH4 becomes upregulated, activating transcriptional programs that support stemness, alter differentiation trajectories, and potentially promote fibrosis and inflammation (a pro-tumorigenic state). This rewiring of the epigenetic landscape enhances tumor plasticity and its immune evasion. While our integrative analyses support a central role for KAT2A in NOTCH-associated chromatin regulation, definitive epistatic relationships between KAT2A and TACC3 will require further functional studies in HCC.

These findings also highlight potential therapeutic avenues in HCC. TACC3 knockdown selectively induces p53-PUMA-mediated apoptosis in cancer cells while not affecting hepatocytes, revealing a putative cancer-specific vulnerability. Targeting key nodes of the FOXM1-DNMT1-KAT2A-TACC3 axis, including FOXM1 to prevent TACC3 upregulation, DNMT1 to restore methylation balance, or disruption of the TACC3-KAT2A interaction, may synergistically impair tumor-specific cell-cycle progression and epigenetic plasticity. While these results provide a mechanistic rationale for intervention, further preclinical studies are

required.

A limitation of our study is the context-dependence of certain validations. While our key findings on the FOXM1-TACC3 and DNMT1-TACC3 axes are substantiated by data from HepG2 cells and *in vivo* by murine liver models, validation of the KAT2A interaction and the ZNF692-KAT2A regulatory relationship rely on data obtained from other cellular contexts than liver. Additional limitations include the lack of inducible or transient DNMT1 perturbation, which could help separate developmental from postnatal effects, and the absence of direct FOXM1-mediated KAT2A recruitment evidence. These constraints may impact the generalizability and causal interpretation of the observed regulatory relationships. Direct experimental confirmation of these interactions in hepatocytic or HCC models is therefore an important direction for future research to solidify their mechanistic relevance in liver cancer.

Together, our findings reveal a multi-layered regulatory architecture in HCC, in which isoform-specific expression of TACC3 integrates transcriptional, epigenetic, and signaling reprogramming. We define a FOXM1-DNMT1-KAT2A-TACC3 axis that orchestrates this rewiring.

Authors' Contribution

L.N.Z, and J.B.A conceived the idea, designed and implemented the study. L.N.Z performed the data analysis. J.B.A provided critical insights, guided the overall direction of the project. Together, they wrote the manuscript.

Acknowledgements

The authors would like to thank the patients and their families for allowing research access to their samples. Also, we are grateful for access to all public datasets. The results are in part supported by data generated by the TCGA Research Network (https://www.cancer.gov/tcga). LNZ would like to express her gratitude for the help from Prof. Mikael Bjorklund and Patrik Midlöv.

The laboratory of JBA is supported by competitive funding from the Novo Nordisk Foundation (0058419, 220C0074956, 0085704), Danish Cancer Society (R98-A6446, R167-A10784, R278-A16638), Independent Research Fund Denmark for Medical Research (4183-00118A, 1030-00070B).

Conflicts of Interest

J.B.A declares consultancies for Flagship Pioneering, QED Therapeutics, and AstraZeneca. J.B.A has received funding from the Incyte Corporation and Adcendo but is not related to this study.

SUPPLEMENTARY MATERIAL

Supplementary material is available at Clinical and Molecular Hepatology website (http://www.e-cmh.org).

REFERENCES

1. Yu L, Kim J, Jiang L, Feng B, Ying Y, Ji KY, et al. MTR4 drives liver tumorigenesis by promoting cancer metabolic switch through alternative splicing. Nat Commun 2020;11:708.
2. Li S, Hu Z, Zhao Y, Huang S, He X. Transcriptome-wide analysis reveals the landscape of aberrant alternative splicing events in liver cancer. Hepatology 2019;69:359-375.
3. Kahles A, Lehmann KV, Toussaint NC, Hüser M, Stark SG, Sachsenberg T, et al. Comprehensive analysis of alternative splicing across tumors from 8,705 patients. Cancer Cell 2018;34:211-224.e6.
4. Robertson KD. DNA methylation and chromatin - unraveling the tangled web. Oncogene 2002;21:5361-5379.
5. Webster NJG, Kumar D, Wu P. Dysregulation of RNA splicing in early non-alcoholic fatty liver disease through hepatocellular carcinoma. Sci Rep 2024;14:2500.
6. Lee SE, Alcedo KP, Kim HJ, Snider NT. Alternative splicing in hepatocellular carcinoma. Cell Mol Gastroenterol Hepatol 2020;10:699-712.
7. Shi S, Guo D, Ye L, Li T, Fei Q, Lin M, et al. Knockdown of TACC3 inhibits tumor cell proliferation and increases chemosensitivity in pancreatic cancer. Cell Death Dis 2023;14:778.
8. Saatci O, Sahin O. TACC3: a multi-functional protein promoting cancer cell survival and aggressiveness. Cell Cycle 2023;22:2637-2655.
9. Lin ZR, Wang MY, He SY, Cai ZM, Huang WR. TACC3 transcriptionally upregulates E2F1 to promote cell growth and confer sensitivity to cisplatin in bladder cancer. Cell Death Dis 2018;9:72.
10. Lyko F. The DNA methyltransferase family: a versatile toolkit for epigenetic regulation. Nat Rev Genet 2018;19:81-92.

11. Chen T, Mahdadi S, Vidal M, Desbène-Finck S. Non-nucleoside inhibitors of DNMT1 and DNMT3 for targeted cancer therapy. Pharmacol Res 2024;207:107328.
12. Laranjeira ABA, Hollingshead MG, Nguyen D, Kinders RJ, Doroshow JH, Yang SX, et al. DNA damage, demethylation and anticancer activity of DNA methyltransferase (DNMT) inhibitors. Sci Rep 2023;13:5964.
13. Nishiyama A, Mulholland CB, Bultmann S, Kori S, Endo A, Saeki Y, et al. Two distinct modes of DNMT1 recruitment ensure stable maintenance DNA methylation. Nat Commun 2020;11:1222.
14. Clements EG, Mohammad HP, Leadem BR, Easwaran H, Cai Y, Van Neste L, et al. DNMT1 modulates gene expression without its catalytic activity partially through its interactions with histone-modifying enzymes. Nucleic Acids Res 2012;40:4334-4346.
15. Lou L, Deng T, Yuan Q, Wang L, Wang Z, Li X, et al. Targeted silencing of SOCS1 by DNMT1 promotes stemness of human liver cancer stem-like cells. Cancer Cell Int 2024;24:206.
16. Hu G, Yan Z, Zhang C, Cheng M, Yan Y, Wang Y, et al. FOXM1 promotes hepatocellular carcinoma progression by regulating KIF4A expression. J Exp Clin Cancer Res 2019;38:188.
17. Wang N, Wu R, Tang D, Kang R. The BET family in immunity and disease. Signal Transduct Target Ther 2021;6:23.
18. Cao X, Liu L, Cao X, Cui Y, Zou C, Chen A, et al. The DNMT1/miR-34a/FOXM1 axis contributes to stemness of liver cancer cells. J Oncol 2020;2020:8978930.
19. Liu R, Zhao E, Yu H, Yuan C, Abbas MN, Cui H, et al. Methylation across the central dogma in health and diseases: new therapeutic strategies. Signal Transduct Target Ther 2023;8:310.
20. Teh MT, Gemenetzidis E, Patel D, Tariq R, Nadir A, Bahta AW, et al. FOXM1 induces a global methylation signature that mimics the cancer epigenome in head and neck squamous cell carcinoma. PLoS One 2012;7:e34329.
21. Zhao Q, Nardo WD, Wang R, Zhong Y, Keles U, Sakalauskaite G, et al. Global molecular landscape of early MASLD progression in obesity. eLife 2025;14:RP109534.
22. Zhao Q, Nardo WD, Wang R, Zhong Y, Keles U, Zhao LN, et al. Omics-based insights into human liver reveal GTPase-driven mechanisms of MASLD progression in obesity. BioRxiv [Preprint]. 2025 [cited 2025 Jan. 14]. Available from: https://doi.org/10.1101/2025.01.13.632747.
23. Lu Y, Yang A, Quan C, Pan Y, Zhang H, Li Y, et al. A single-cell atlas of the multicellular ecosystem of primary and metastatic hepatocellular carcinoma. Nat Commun 2022;13:4594.
24. Ma L, Heinrich S, Wang L, Keggenhoff FL, Khatib S, Forgues M, et al. Multiregional single-cell dissection of tumor and immune cells reveals stable lock-and-key features in liver cancer. Nat Commun 2022;13:7533.
25. Lee SHT, Garske KM, Arasu UT, Kar A, Miao Z, Alvarez M, et al. Single nucleus RNA-sequencing integrated into risk variant colocalization discovers 17 cell-type-specific abdominal obesity genes for metabolic dysfunction-associated steatotic liver disease. EBioMedicine 2024;106:105232.
26. Alvarez M, Benhammou JN, Darci-Maher N, French SW, Han SB, Sinsheimer JS, et al. Human liver single nucleus and single cell RNA sequencing identify a hepatocellular carcinoma-associated cell-type affecting survival. Genome Med 2022;14:50.
27. Darci-Maher N, Alvarez M, Arasu UT, Selvarajan I, Lee SHT, Pan DZ, et al. Cross-tissue omics analysis discovers ten adipose genes encoding secreted proteins in obesity-related non-alcoholic fatty liver disease. EBioMedicine 2023;92:104620.
28. Lafita-Navarro MC, Hao YH, Jiang C, Jang S, Chang TC, Brown IN, et al. ZNF692 organizes a hub specialized in 40S ribosomal subunit maturation enhancing translation in rapidly proliferating cells. Cell Rep 2023;42:113280.
29. ENCODE Project Consortium. An integrated encyclopedia of DNA elements in the human genome. Nature 2012;489:57-74.
30. Kaji K, Factor VM, Andersen JB, Durkin ME, Tomokuni A, Marquardt JU, et al. DNMT1 is a required genomic regulator for murine liver histogenesis and regeneration. Hepatology 2016;64:582-598.
31. Vitting-Seerup K, Sandelin A. IsoformSwitchAnalyzeR: analysis of changes in genome-wide patterns of alternative splicing and its functional consequences. Bioinformatics 2019;35:4469-4471.
32. Vitting-Seerup K, Sandelin A. The landscape of isoform switches in human cancers. Mol Cancer Res 2017;15:1206-1220.
33. Reyes A, Anders S, Weatheritt RJ, Gibson TJ, Steinmetz LM, Huber W, et al. Drift and conservation of differential exon usage across tissues in primate species. Proc Natl Acad Sci U S A 2013;110:15377-15382.
34. Anders S, Reyes A, Huber W. Detecting differential usage of exons from RNA-seq data. Genome Res 2012;22:2008-2017.
35. Gilis J, Vitting-Seerup K, Van den Berge K, Clement L. SatuRn: scalable analysis of differential transcript usage for bulk and single-cell RNA-sequencing applica-

tions. F1000Res 2021;10:374.
36. Love MI, Huber W, Anders S. Moderated estimation of fold change and dispersion for RNA-seq data with DESeq2. Genome Biol 2014;15:550.
37. Efremova M, Vento-Tormo M, Teichmann SA, Vento-Tormo R. CellPhoneDB: inferring cell-cell communication from combined expression of multi-subunit ligand-receptor complexes. Nat Protoc 2020;15:1484-1506.
38. Jin S, Plikus MV, Nie Q. CellChat for systematic analysis of cell-cell communication from single-cell transcriptomics. Nat Protoc 2025;20:180-219.
39. Aryee MJ, Jaffe AE, Corrada-Bravo H, Ladd-Acosta C, Feinberg AP, Hansen KD, et al. Minfi: a flexible and comprehensive Bioconductor package for the analysis of Infinium DNA methylation microarrays. Bioinformatics 2014;30:1363-1369.
40. Zatzman M, Fuligni F, Ripsman R, Suwal T, Comitani F, Edward LM, et al. Widespread hypertranscription in aggressive human cancers. Sci Adv 2022;8:eabn0238.
41. Phoolchund AGS, Khakoo SI. MASLD and the development of HCC: pathogenesis and therapeutic challenges. Cancers (Basel) 2024;16:259.
42. Nepal C, Andersen JB. Alternative promoters in CpG depleted regions are prevalently associated with epigenetic misregulation of liver cancer transcriptomes. Nat Commun 2023;14:2712.
43. Zhang Y, Qian J, Gu C, Yang Y. Alternative splicing and cancer: a systematic review. Signal Transduct Target Ther 2021;6:78.
44. Saatci O, Akbulut O, Cetin M, Sikirzhytski V, Uner M, Lengerli D, et al. Targeting TACC3 represents a novel vulnerability in highly aggressive breast cancers with centrosome amplification. Cell Death Differ 2023;30:1305-1319.
45. Gangisetty O, Lauffart B, Sondarva GV, Chelsea DM, Still IH. The transforming acidic coiled coil proteins interact with nuclear histone acetyltransferases. Oncogene 2004;23:2559-2563.
46. Zender S, Nickeleit I, Wuestefeld T, Sörensen I, Dauch D, Bozko P, et al. A critical role for notch signaling in the formation of cholangiocellular carcinomas. Cancer Cell 2013;23:784-795.
47. Lewinska M, Kårhus ML, Ellegaard AG, Romero-Gómez M, Macias RIR, Andersen JB, et al. Serum lipidome unravels a diagnostic potential in bile acid diarrhoea. Gut 2023;72:1698-1708.
48. González-Romero F, Mestre D, Aurrekoetxea I, O'Rourke CJ, Andersen JB, Woodhoo A, et al. E2F1 and E2F2-mediated repression of CPT2 establishes a lipid-rich tumor-promoting environment. Cancer Res 2021;81:2874-2887.
49. Saatci O, Akbulut O, Cetin M, Sikirzhytski V, Uner M, Lengerli D, et al. Abstract PO4-24-04: identifying the interactome of TACC3, a major driver in aggressive cancer cells with centrosome amplification. Res 2024;84:PO4-24-04.

https://doi.org/10.3350/cmh.2025.1370